THE ASTROPHYSICAL JOURNAL, 320:803–817, 1987 September 15

COLLISIONAL CHARGING OF INTERSTELLAR GRAINS

B. T. DRAINE AND BRIAN SUTIN
Princeton University Observatory
Received 1986 November 24; accepted 1987 March 2

ABSTRACT

Collisional charging of small interstellar particles is reexamined, including effects due to electrostatic polarization of the grain by the electric field of an approaching charged particle. Energy-dependent capture cross sections are derived for spherical particles, and these cross sections are convolved with thermal velocity distributions to obtain rate coefficients for electron and ion collisions with spherical grains of arbitrary size and charge state. The polarization interaction leads to significant modifications in charging rates when the grain charge is small. The probability distribution for the grain charge is obtained for the case of pure collisional charging (i.e., photoelectric emission due to background ultraviolet is neglected); the distribution functions depend on only two dimensionless parameters: the "reduced temperature" $\tau \propto aT$ (where a is the grain radius and T is the kinetic temperature of the plasma), and the "effective atomic weight" μ of the ions, which depends not only on the masses of the ions but also on the electron sticking coefficient and the ratio n_e/n_i. Approximate formulae are obtained for both the average grain charge and the average rate of collisions with ions. The average grain charge and average collision rate are also integrated over a grain size distribution to estimate the total charge carried by the grain population, and to obtain an effective "grain recombination coefficient" for ions. For the MRN grain size distribution (extended down to $a_{\min} \approx 3$ Å) it is found that recombination on grain surfaces is faster than radiative recombination in dark clouds when the fractional ionization $n_e/n_H \lesssim 10^{-2}$, indicating that recombination on grain surfaces may be the principal destruction process for ions such as Mg^+ and S^+ in dark clouds. Even for ions subject to rapid dissociative recombination, recombination on grain surfaces can be faster when $n_e/n_H \lesssim 10^{-7}$.

Subject headings: atomic processes — interstellar: grains — molecular processes

I. INTRODUCTION

Interstellar grains are commonly charged, and the charge on the grain can have important consequences for both the grain and the interstellar gas in which the grain is found. The grain charge is often sufficient for the grain to be strongly coupled to the magnetic field. When the fractional ionization in the gas becomes very small, charged dust grains can actually become the dominant agent for coupling the magnetic field to the neutral gas, a fact which has important consequences for estimation of the rate of ambipolar diffusion in the cores of dense molecular clouds (Elmegreen 1979; Nakano and Umebayashi 1980). The charge state of grains in dark clouds affects the rate at which atoms, ions, and electrons collide with the grains; under some circumstances, ions may recombine more rapidly by colliding with negatively charged grains than by radiatively recombining with free electrons (Mestel and Spitzer 1956; Nakano and Tademaru 1972; Watson 1974; Nakano 1976; Elmegreen 1979; Umebayashi and Nakano 1980). Finally, the charge state on a grain affects the rate of photoelectric emission; in order to improve previous estimates of the rate of photoelectric charging of grains and heating of interstellar gas, particularly for very small grains, it is important to treat the collisional charging processes accurately.

This paper revisits what at first sight seems familiar territory: collisional charging of interstellar dust by low-energy ($\lesssim 10$ eV) electrons and ions. This subject has been previously studied by a number of authors (e.g., Spitzer 1941; see the recent review by Havnes 1984). A reinvestigation of the physics of this process is motivated by the recognition that previous studies of this problem have neglected the polarization of the dust grain by the approaching electron or ion; associated with this polarization is an attractive force. While this effect is indeed relatively minor for "classical" ($a \gtrsim 0.1$ μm) interstellar grains at "high" ($T \gtrsim 100$ K) temperatures, it can have profound consequences for very small grains or at very low temperatures.

Interest in the astrophysics of very small particles has been stimulated by recent circumstantial evidence pointing to the presence in interstellar clouds of large numbers of very small particles, consisting of as few as 30 or so atoms. Some of these particles appear to have the chemical structure of "polycyclic aromatic hydrocarbons" or "PAHs" (Leger and Puget 1984). Whether one chooses to refer to such entities as "grains" or as "molecules" is largely a matter of convention, although it is obvious that in some respects the physical properties of such particles may differ significantly from those of "bulk" material. Omont (1986) has recently examined, from a "molecular" viewpoint, the physics of PAHs in interstellar gas. In this paper we consider the collisional charging of grains, modeling them as conducting spheres, and consider grain radii as small as $a \approx 3$ Å.

In § II we discuss the interaction potential and resulting energy-dependent collision cross section. This cross section is used in § III to obtain the collisional charging rate for a grain of specified charge in a thermal plasma. The probability distribution for the grain charge is obtained in § IV. Our results are discussed in § V, where we illustrate their application to the interstellar medium by considering the "MRN" power-law grain size distribution of Mathis, Rumpl, and Nordsieck (1977). In particular, we find that dust grains with such a size distribution can contribute appreciably to the recombination of metal ions in dark clouds. Our results are summarized in § VI.

II. COLLISION CROSS SECTIONS

a) Interaction Potential

Consider a spherical grain of radius a and charge Ze. We assume that the grain may be approximated as a perfect conductor. The force acting on a charge q located a distance r from the center of the conducting sphere may be derived from the interaction potential

$$\Phi(Z, r) = \frac{qZe}{r} - \frac{q^2a^3}{2r^2(r^2 - a^2)} \tag{2.1}$$

(cf. eq. [2.9] of Jackson 1962). The first term in equation (2.1) is the familiar monopole-monopole interaction; the second term is the "image potential" resulting from the polarization of the grain induced by the Coulomb field of the charge q.

We have assumed that the grain may be modeled as a conducting sphere. While this appears to limit the present treatment to the case of grains composed of conducting materials (e.g., graphite), the polarization of a dielectric grain with an appreciable dielectric constant ($\epsilon \gtrsim 5$) results in an electric field outside the grain which closely resembles that for a conducting grain (for which $\epsilon \to \infty$). As shown in Appendix A, the polarization interaction for a dielectric grain is essentially proportional to that for a conducting grain, with proportionality factor $\sim(\epsilon - 1)/(\epsilon + 2)$; this factor exceeds 0.57 for $\epsilon > 5$. Candidate dielectric grain materials are expected to have zero-frequency dielectric constant $\epsilon \gtrsim 5$ (the silicate mineral olivine, for example, has $\epsilon \approx 7$; Touloukian and Ho 1981). The present analysis for conducting spheres is therefore a good approximation to the behavior of spherical dielectric grains.

For future reference, we note that in the case of a repulsive long range potential ($Zeq > 0$) the maximum of $\Phi(Z, r)$ occurs at $r = \xi_\nu a$, where $\xi_\nu > 1$ is a root of

$$2\xi_\nu{}^2 - 1 - \nu\xi_\nu(\xi_\nu{}^2 - 1)^2 = 0 \tag{2.2}$$

$$\nu \equiv Ze/q . \tag{2.3}$$

For singly-charged ions ($q = e$) or electrons ($q = -e$), ν takes on only integral values. (Note, however, that fractional values of ν would be of interest in considering collisions of multiply charged ions with grains.) Values of ξ_ν are given in Table 1 for selected values of ν, together with values of

$$\theta_\nu \equiv \frac{\Phi(r = \xi_\nu a)}{q^2/a} = \frac{\nu}{\xi_\nu} - \frac{1}{2\xi_\nu{}^2(\xi_\nu{}^2 - 1)} ; \tag{2.4}$$

TABLE 1

FUNCTIONS ξ_ν AND θ_ν

ν	ξ_ν	θ_ν/ν
≤0	...	0
0.5	1.8822	0.4203
1	1.6180	0.5000
2	1.4276	0.5823
3	1.3434	0.6296
4	1.2936	0.6621
5	1.2600	0.6865
10	1.1783	0.7560
20	1.1226	0.8146

θ_ν is a dimensionless measure of the value of the potential maximum. It is convenient to define $\theta_\nu = 0$ for $\nu \leq 0$. An excellent approximation to θ_ν is provided by

$$\theta_\nu \approx \frac{\nu}{1 + \nu^{-1/2}} ; \tag{2.4a}$$

this formula is accurate to within 0.7% for $1 \leq \nu < \infty$.

At large separations $r \gg a$ the "image potential" term in Φ varies as $-q^2a^3/2r^4$, corresponding to a polarizability $\alpha = a^3$ for the sphere. It is interesting to compare this polarizability estimate for a very small grain with that expected from a molecular viewpoint. Consider, for example, a grain with $a = 4$ Å, containing $N \approx 30$ atoms, for which we estimate $\alpha = 6.4 \times 10^{-23}$ cm^3. Omont (1986) has estimated the polarizability of a 30 carbon atom "circular" PAH to be $\alpha = 1.5 \times 10^{-22}$ cm^3, somewhat larger than our estimate because we have assumed a spherical grain while Omont considers a two-dimensional PAH. In view of the apparent continuity of the molecular and continuum viewpoints, it appears that we may confidently extend our "continuum" estimate of the interaction potential down into the molecular regime.

b) Capture Cross Section

Consider a charge q with kinetic energy E (at infinity). The cross section for a collision with the grain surface is given by (see Appendix B)

$$\sigma(q, Z, a, E) \equiv \pi a^2\tilde{\sigma}(\epsilon, \nu) \tag{2.5}$$

where

$$\epsilon \equiv \frac{Ea}{q^2} , \tag{2.6}$$

$$\nu \equiv \frac{Ze}{q} . \tag{2.7}$$

Clearly $\nu > 0$ for a repulsive Coulomb potential, $\nu = 0$ for an uncharged grain, and $\nu < 0$ for an attractive Coulomb interaction. The "reduced" cross section $\tilde{\sigma}(\epsilon, \nu)$ is given by (see Appendix B)

$$\tilde{\sigma}(\epsilon, \nu) = x^2 + \frac{1}{\epsilon}\left[\frac{1}{2(x^2 - 1)} - \nu x\right] \quad \text{for } \epsilon > \theta_\nu , \tag{2.8}$$

$$\tilde{\sigma}(\epsilon, \nu) = 0 \quad \text{for } \epsilon \leq \theta_\nu , \tag{2.9}$$

where $x > 1$ is a root of the equation

$$(2\epsilon x - \nu)(x^2 - 1)^2 - x = 0 . \tag{2.10}$$

Analytic results are readily obtained for the special case of a neutral grain ($\nu = 0$):

$$\tilde{\sigma}(\epsilon, \nu = 0) = 1 + \left(\frac{2}{\epsilon}\right)^{1/2} . \tag{2.11}$$

Note that for low energies $\epsilon \ll 1$ this has the property that $\tilde{\sigma} \propto \epsilon^{-1/2}$, or $\sigma v =$ constant, just as for the case of low energy ion-molecule scattering.

In the limit $|\nu| \to \infty$ (i.e., the limit of a large grain with many quanta of excess charge) one can expand in powers of $|\nu|^{-1/2}$ to obtain

$$\tilde{\sigma}(\epsilon, \nu \gg 1) \approx 1 - \frac{\nu}{\epsilon} + \frac{(2\epsilon - \nu)^{1/2}}{\epsilon} + O(\nu^{-1}) . \tag{2.12}$$

(In examining the asymptotic behavior as $\nu \to \infty$, note that since $\theta_\nu \to \nu$, the dimensionless energy $\epsilon \propto \nu$. Note also that since $\epsilon > \theta_\nu$ and $\theta_\nu \geq \nu/2$ for $\nu \geq 1$, the term $(2\epsilon - \nu)$ is non-negative.) In the limit $\nu \to \infty$ one has $\sigma \to 1 - \nu/\epsilon$, the classic result obtained by Spitzer (1941).

For the case of general interest, where ν is neither zero nor very large, $\tilde{\sigma}(\epsilon, \nu)$ must be obtained by numerically solving the quintic equation (2.10) for $x(\epsilon, \nu)$; $x(\epsilon, \nu)$ is then substituted into eq. (2.8) to obtain $\tilde{\sigma}(\epsilon, \nu)$. Results are shown in Figure 1, for selected values of the charge ratio ν.

c) *Sticking Coefficients*

When an electron reaches the grain surface, it has some probability of being reflected from (or transmitted through) the grain with enough energy to escape to infinity; this probability depends upon the energy of the approaching electron, the radius a and composition of the grain, and the charge Ze on the grain. Let the "electron sticking coefficient" $s_e(a, Z, T) < 1$ denote the average probability that a colliding electron will "stick" to the grain and eventually be trapped in a bound state of either the grain substrate or an adsorbed ion. In addition to depending on the grain properties, s_e is a function of the plasma temperature T, since this affects the distribution of kinetic energies of the impinging electrons.

For grains in cold clouds, Umebayashi and Nakano (1980) have argued that $s_e \approx 1$. This conclusion was based on a theoretical analysis of the excitation of phonons by the electron as it "hops" translationally along the grain surface. This result was supported by laboratory studies of graphite (Lander and Morrisson 1964), KCl and KBr (Fredericks and Cook 1961), and NaCl (Fredericks and Cook 1963), which found $s_e \approx 0.3$ for electron energies $E \approx 1$ eV. Here we note only that the analysis of Umebayashi and Nakano (1980), based on the model of Hollenbach and Salpeter (1970), assumes a planar grain surface; curvature of the grain surface will tend to reduce the sticking coefficient, possibly leading to a significant reduction in the electron sticking coefficient for very small ($a \lesssim 10$ Å) grains. Because of this uncertainty, we will leave s_e as an adjustable parameter in our formulae below.

The sticking probability for ions is almost certainly close to unity. If the impinging ion (e.g., H^+ or C^+) has an ionization potential which is significantly in excess of the work function of the grain material, an electron from the grain will quickly tunnel into a bound energy level and neutralize the ion; the resulting atom may or may not remain adsorbed to the grain, but this is of no consequence so far as the charge state of the grain is concerned.

Even if the impinging ion has a small ionization potential (e.g., Na^+), the impinging ion can readily lose enough kinetic energy to the lattice (i.e., excite phonons) so that it becomes trapped by the image potential. Once trapped on the grain surface, such an ion may remain as an adsorbed ion. Accordingly, we shall assume the sticking coefficient to be unity for ions.

III. THERMAL RATES

a) *Collisional Charging Rate*

Let $J_i(Z)$ be the rate at which charged particles with number density n_i, charge q_i, mass m_i, and sticking coefficient s_i arrive at the grain surface. If the charged particles have a Maxwellian distribution at infinity, then

$$J_i(Z) = n_i s_i \left(\frac{8kT}{\pi m_i}\right)^{1/2} \pi a^2 \tilde{J}\left(\tau = \frac{akT}{q_i^2}, \nu = \frac{Ze}{q_i}\right), \quad (3.1)$$

where $\tau \equiv akT/q_i^2$ is the "reduced temperature," and

$$\tilde{J}(\tau, \nu) \equiv \int_0^\infty dx\, x\, e^{-x} \tilde{\sigma}(\epsilon = x\tau, \nu) . \quad (3.2)$$

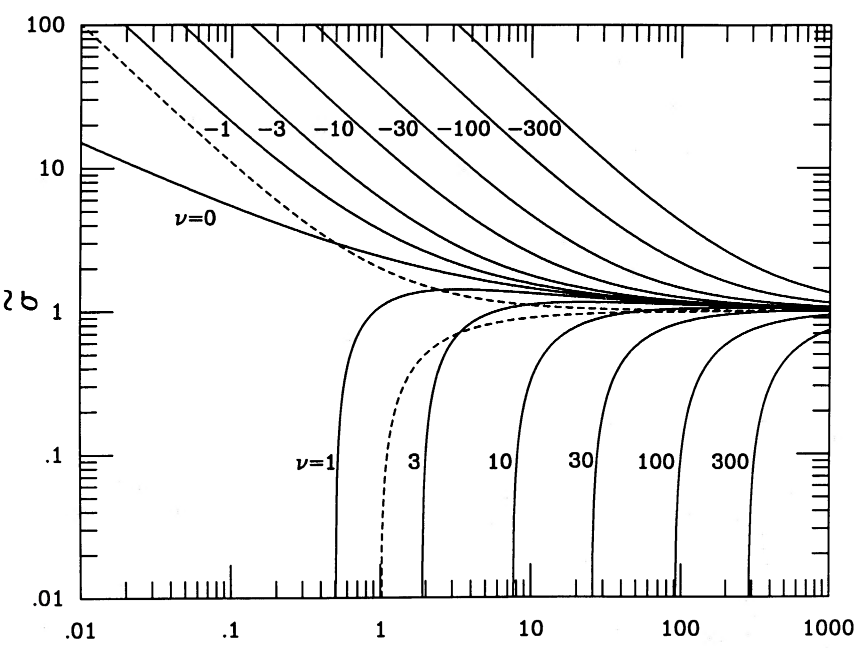

FIG. 1.—The reduced collision cross section $\tilde{\sigma}(\epsilon, \nu)$, as a function of $\epsilon \equiv Ea/q^2$. The actual cross section is just $\tilde{\sigma}\pi a^2$, where a is the grain radius. Curves are labeled by values of $\nu \equiv Ze/q$, the ratio of the charge on the grain to the charge q of the incident particle. For comparison, the broken curves show the "classical" result $\tilde{\sigma} = 1 - \nu/\epsilon$, for $\nu = +1$ and -1.

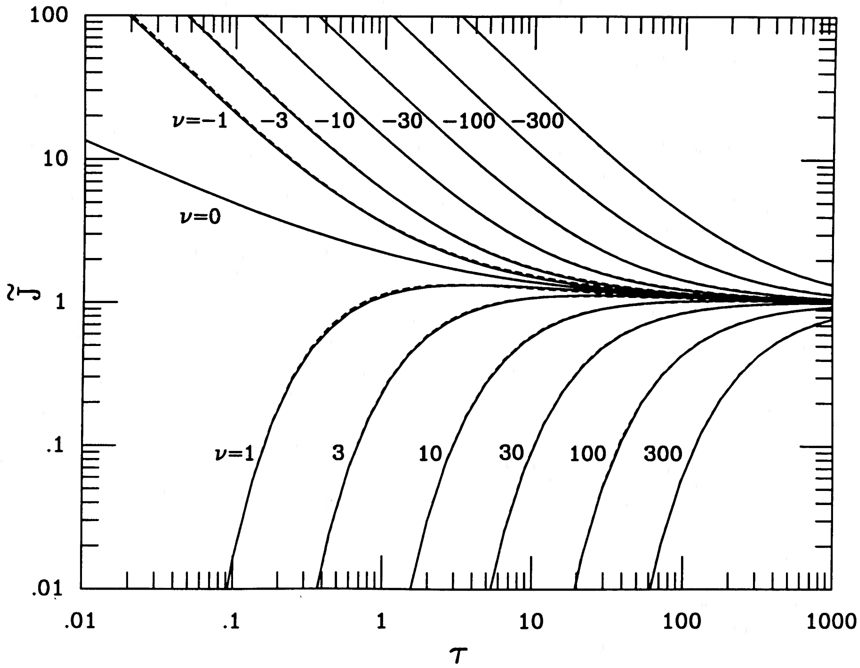

FIG. 2.—The reduced rate coefficient $\tilde{J}(\tau, \nu)$, as a function of the reduced temperature $\tau \equiv akT/q^2$, where a is the grain radius and q is the charge on the incident particle. Curves are labeled by values of $\nu \equiv Ze/q$, the ratio of the charge on the grain to the charge on the incident particle. The solid curves are exact; the broken curves are the approximate formulae (3.4) and (3.5) for $\nu < 0$ and $\nu > 0$, respectively. For $|\nu| > 3$ the approximate formulae are nearly indistinguishable from the exact results on this plot.

The function $\tilde{J}(\tau, \nu)$ is plotted in Figure 2 as a function of the reduced temperature τ, for selected values of ν.

The special case $\nu = 0$ (i.e., neutral grain) yields the simple result

$$\tilde{J}(\tau, \nu = 0) = 1 + \left(\frac{\pi}{2\tau}\right)^{1/2} . \qquad (3.3)$$

For the case of $\nu < 0$ (attractive Coulomb potential at large distances) we note that $\tilde{\sigma} \to 1$ for $\epsilon \to \infty$, but $\tilde{\sigma} \to \infty$ for $\epsilon \to 0$. It is helpful to think of the electrostatic focusing as consisting of two distinct stages: (1) long-range Coulomb focusing, which enhances the capture cross section by the familiar factor $(1 - Zeq/akT) = (1 - \nu/\tau)$; (2) short-range focusing by the polarization interaction, which enhances the capture cross section by a factor (see eq. [2.11]) $[1 + (2q^2/E'a)^{1/2}]$, where E' is the kinetic energy which the (Coulomb-focused) charged particle has as it approaches the region where the polarization interaction becomes effective. It turns out that a very good fit is obtained by setting $E' \approx kT - 2Zeq/a$, in which case we obtain the approximate formula

$$\tilde{J}(\nu < 0) \approx \left[1 - \frac{\nu}{\tau}\right]\left[1 + \left(\frac{2}{\tau - 2\nu}\right)^{1/2}\right] . \qquad (3.4)$$

This formula reproduces our numerical results to within $\pm 5\%$ for $10^{-3} < \tau < \infty$ and $\nu \leq -1$.

For $\nu > 0$ (repulsive long-range Coulomb interaction), we expect $\tilde{J} \to 1$ for $\tau \to \infty$ and $\tilde{J} \propto \xi_\nu^2 \exp(-\theta_\nu/\tau)$ for $\tau \to 0$, where ξ_ν is defined by equation (2.2) (recall that $\xi_\nu a$ is the radius at which the interaction potential peaks). A simple fitting formula for ξ_ν is $\xi_\nu \approx 1 + (3\nu)^{-1/2}$ (accurate to within 2.5% for $\nu \geq 1$). A simple formula for $\tilde{J}$ which fits well for all τ is

$$\tilde{J}(\nu > 0) \approx [1 + (4\tau + 3\nu)^{-1/2}]^2 \exp(-\theta_\nu/\tau) . \qquad (3.5)$$

Equation (3.5) is accurate to within $\pm 4\%$ for $\nu \geq 1$.

b) *Collisional Cooling*

Charged particles colliding with (and sticking to) the grain remove thermal energy from the plasma at a rate (per grain) given by (assuming the sticking coefficient s_i to be energy-independent)

$$\Lambda_i(Z) = n_i s_i \left(\frac{8kT}{\pi m_i}\right)^{1/2} \pi a^2 kT \tilde{\Lambda}\left(\tau = \frac{akT}{q_i^2}, \nu = \frac{Ze}{q_i}\right) , \qquad (3.6)$$

where

$$\tilde{\Lambda} \equiv \int_0^\infty dx\, x^2 e^{-x} \tilde{\sigma}(\epsilon = x\tau, \nu) . \qquad (3.7)$$

For the special case $\nu = 0$ we have the exact result

$$\tilde{\Lambda} = 2 + \frac{3}{2}\left(\frac{\pi}{2\tau}\right)^{1/2} . \qquad (3.8)$$

For $\nu < 0$ we find that our numerical results may be approximated by the fitting formula

$$\tilde{\Lambda}(\nu < 0) \approx \left[2 - \frac{\nu}{\tau}\right][1 + (\tau - \nu)^{-1/2}] , \qquad (3.9)$$

accurate to within $\pm 10\%$ for $\tau > 10^{-1}$, while for $\nu > 0$ a satisfactory fit is provided by

$$\tilde{\Lambda}(\nu > 0) \approx \left[2 + \frac{\nu}{\tau}\right]\left[1 + \left(\frac{3}{2\tau} + 3\nu\right)^{-1/2}\right] \exp\left(-\frac{\theta_\nu}{\tau}\right) , \qquad (3.10)$$

accurate to within $\pm 5\%$ for $\tau > 10^{-3}$. In Figure 3 we show the exact results for $\tilde{\Lambda}$ for selected values of ν, as well as the approximate formulae (3.9) and (3.10). It is seen that the approximate formulae give an excellent approximation for $\tilde{\Lambda}$.

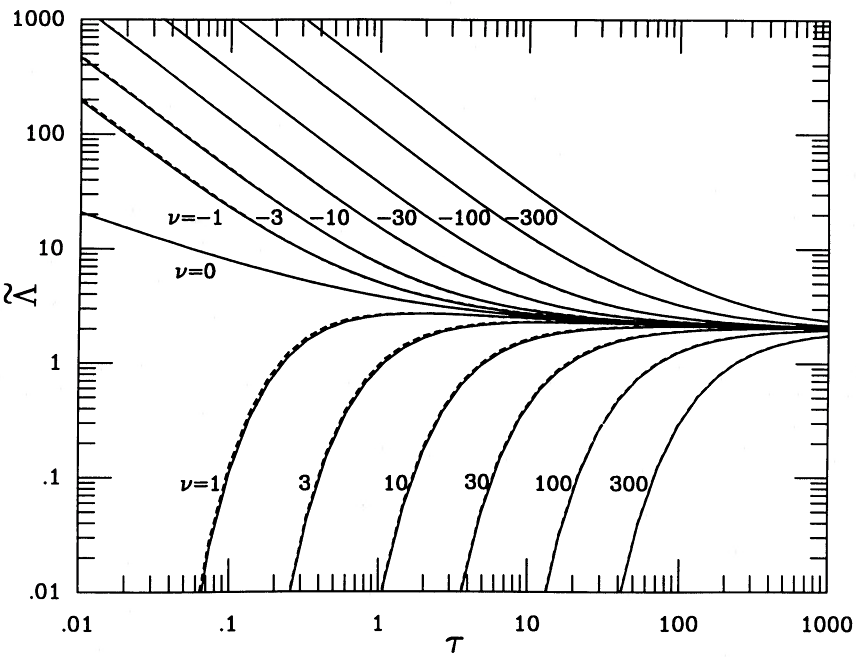

FIG. 3.—The reduced cooling rate $\tilde{\Lambda}(\tau, \nu)$, as a function of the reduced temperature $\tau \equiv akT/q^2$. Curves are labeled by values of ν, the ratio of the charge on the grain to the charge on the incident particle. Solid curves show the exact results; broken curves show the approximate formulae (3.9) and (3.10) for $\nu < 0$ and $\nu > 0$, respectively.

The mean thermal energy per colliding particle is

$$\frac{\Lambda}{J} = \frac{\tilde{\Lambda}}{\tilde{J}} kT \tag{3.11}$$

and is plotted in Figure 4. It is seen that for the purely attractive potentials ($\nu \leq 0$), the mean energy per colliding particle is always between kT and $2kT$. Only in the case of repulsive interactions and "low" temperatures ($\tau \lesssim \nu/3$) does the mean energy per colliding particle begin to rise significantly above $2kT$, since only the most energetic particles are able to surmount the repulsive barrier to reach the grain surface; however, in these cases both $\tilde{J}$ and $\tilde{\Lambda}$ are small.

IV. CHARGE DISTRIBUTION FOR SMALL PARTICLES

a) *Field Emission Processes and Maximum Grain Charge*

i) *Electron Field Emission*

When an interstellar grain becomes highly negatively charged, it may be energetically favorable for an electron in the

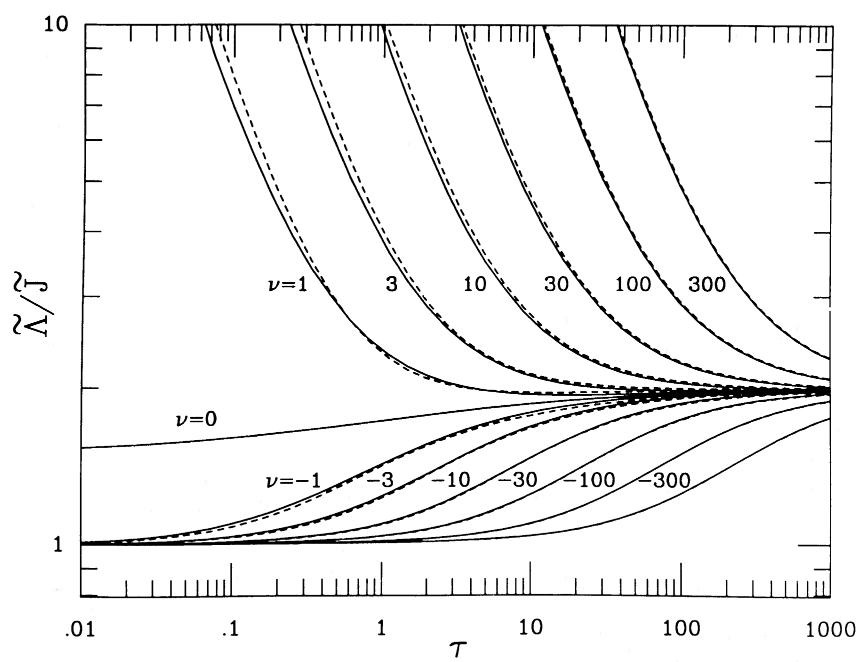

FIG. 4.—The mean energy (at infinity) of the colliding particles, in units of kT, as a function of the reduced temperature $\tau \equiv akT/q^2$. Curves are labeled by values of ν, the ratio of the charge on the grain to the charge on the incident particle. Solid curves show the exact results; broken curves are obtained from eq. (3.4) and (3.9) for $\nu < 0$, and (3.5) and (3.10) for $\nu > 0$.

grain to be removed to infinity. To accomplish this, however, the electron must tunnel through a classically forbidden region just outside the solid surface. Quantum tunnelling calculations as well as experimental studies indicate that the tunnelling rate becomes appreciable when the electric field at the surface of the sample exceeds $\sim 1 \times 10^7$ V cm^{-1} in magnitude (Gomer 1961). This tunnelling phenomenon is referred to as "electron field emission." Consider a grain with initial charge Ze. Taking into account the fact that the electron being removed from the grain interacts with a charge $(Z+1)e$, this implies that electron field emission limits the excess charge on a grain of radius a to

$$Z > -1 - 0.7\left(\frac{a}{10\ \text{Å}}\right)^2 \tag{4.1}$$

ii) *Ion Field Emission*

When the electric field at the surface of a positively charged sample exceeds $\sim 3 \times 10^8 V$ cm^{-1}, it is found that atoms from the grain surface are spontaneously emitted as positive ions (Muller and Tsong 1969). This implies that the excess charge on a small grain is limited to

$$Z < 1 + 21\left(\frac{a}{10\ \text{Å}}\right)^2 \tag{4.2}$$

b) *Kinetic Equations and Limiting Behavior*

Consider a grain of radius a. Let $f(Z)$ be the probability of finding the grain with a net charge Ze. If we neglect processes which change the grain charge by more than a single charge quantum (i.e., we neglect multiply ionized ions such as He^{++}), then f satisfies the equation

$$f(Z)[J_{\text{pe}}(Z) + J_{\text{ion}}(Z)] = f(Z+1)J_e(Z+1)\ , \tag{4.3}$$

where J_{ion} is the rate of collisions with ions, J_e is the rate of collisions with electrons, and J_{pe} is the rate of emission of photoelectrons. The collision rates J_{ion} and J_e are given by equation (3.1). In the present paper we will consider the case where photoelectric charging is negligible, and will set $J_{\text{pe}} = 0$. The effects of photoelectric emission will be examined in a subsequent paper (Draine and Sutin 1987).

In order to obtain $f(Z)$, we successively apply equation (4.3) to, say, $f(0)$; thus

$$f(Z > 0) = f(0) \prod_{Z'=1}^{Z} \left[\frac{J_{\text{pe}}(Z'-1) + J_{\text{ion}}(Z'-1)}{J_e(Z')}\right], \tag{4.4a}$$

$$f(Z < 0) = f(0) \prod_{Z'=Z}^{-1} \left[\frac{J_e(Z'+1)}{J_{\text{pe}}(Z') + J_{\text{ion}}(Z')}\right], \tag{4.4b}$$

where the multiplicative constant $f(0)$ is determined by the normalization condition

$$\sum_{-\infty}^{\infty} f(Z) = 1\ . \tag{4.5}$$

It is seen from equation (4.4) that the charge distribution $f(Z)$ depends only on the *ratios* of the "forward" rates $[J_{\text{pe}}(Z-1) + J_{\text{ion}}(Z-1)]$ to the "reverse" rates $J_e(Z)$. In the limit of pure collisional charging ($J_{\text{pe}} \to 0$), these ratios of rates become (assuming singly charged ions)

$$\frac{J_{\text{ion}}(Z-1)}{J_e(Z)} = \frac{\sum_j (n_{I,j} m_{I,j}^{-1/2})}{n_e s_e m_e^{-1/2}} \frac{\tilde{J}(\tau, \nu = Z-1)}{\tilde{J}(\tau, \nu = -Z)}\ , \tag{4.6}$$

where the summation runs over the different ion species. Thus (aside from their explicit dependence on Z) these rate ratios depend *only* upon (1) the reduced temperature τ, and (2) the composition of the plasma. The results are independent of the plasma density, and the kinetic temperature T and the grain radius a enter only through the single combination $\tau = akT/e^2$. Furthermore, if we let

$$n_I \equiv \sum_j n_{I,j} \tag{4.7}$$

and define the average ion mass m_I by

$$m_I^{-1/2} \equiv n_I^{-1} \sum_j n_{I,j} m_{I,j}^{-1/2}\ , \tag{4.8a}$$

then the plasma composition enters only through the dimensionless ratio $(n_I/n_e s_e)(m_e/m_I)^{1/2}$. We may define an "effective atomic weight" for the ions

$$\mu \equiv \left(\frac{n_e s_e}{n_I}\right)^2 \left(\frac{m_I}{m_p}\right), \tag{4.8b}$$

where $m_p = 1836.1 m_e$ is the proton mass. We explicitly allow for the possibility that $n_I \neq n_e$ since for very low fractional ionizations the grains themselves may carry an appreciable fraction of the free charge.

In the low-τ limit the charge probability distribution $f(Z)$ is concentrated in the two charge states $Z = -1$ and 0. It is straightforward to obtain analytic results [using the approximation (3.4) for $\tilde{J}(\nu = -1)$]:

$$f(0) \approx \left[1 + \left(\frac{\mu m_p}{m_e}\right)^{1/2} \left(1 + \frac{m_e}{\mu m_p}\right) \left(\frac{\pi\tau}{8}\right)^{1/2} \times \frac{1 + (2\tau/\pi)^{1/2}}{1+\tau} \left(1 + \frac{\tau}{8}\right)\right]^{-1}, \tag{4.9}$$

$$f(-1) = f(0) \left(\frac{\mu m_p}{m_e}\right)^{1/2} \left(\frac{\pi\tau}{8}\right)^{1/2} \frac{1 + (2\tau/\pi)^{1/2}}{1+\tau} \left(1 + \frac{\tau}{8}\right), \tag{4.10}$$

and

$$f(+1) = \left(\frac{m_e}{\mu m_p}\right) f(-1)\ . \tag{4.11}$$

Equation (4.9) is accurate whenever the probability distribution is strongly concentrated in the three charge states -1, 0, $+1$; this is the case for $\tau \lesssim 0.2$ (see Figs. 5 and 6 below). For $\tau \lesssim 0.2$, one can satisfactorily approximate (4.9) and (4.10) by

$$f(0) \approx [1 + (\tau/\tau_0)^{1/2}]^{-1} \tag{4.12}$$

and

$$f(-1) \approx [1 + (\tau_0/\tau)^{1/2}]^{-1}\ , \tag{4.13}$$

where

$$\tau_0 \equiv \frac{8}{\pi\mu} \left(\frac{m_e}{m_p}\right) = 1.39 \times 10^{-3} \mu^{-1}\ . \tag{4.14}$$

This characteristic reduced temperature τ_0 is the reduced temperature for which the rate for ions to collide with a grain of charge $Z = -1$ is equal to the rate for electrons to collide with a neutral grain. Thus, for $\tau = \tau_0$ one has $f(-1) = f(0)$. At temperatures $\tau < \tau_0$ the strong coulomb focusing leads to rapid neutralization of grains with $Z = -1$, and $f(0) > f(-1)$: the dominant charge state is $Z = 0$. For $\tau_0 < \tau \lesssim 0.2$, the dominant charge state is $Z = -1$.

In the limit $\tau \to \infty$ (large grains, high temperatures) $f(Z)$ approaches a Gaussian

$$f(Z) \to (2\pi\sigma_Z)^{-1/2} \exp\left[-(Z - \langle Z\rangle)^2/2\sigma_Z^2\right] . \quad (4.15)$$

The position of the peak of the Gaussian is determined by the condition

$$\mu^{1/2}\left(\frac{m_p}{m_e}\right)^{1/2} \tilde{J}(\tau, -Z) = \tilde{J}(\tau, +Z) . \quad (4.16)$$

In the limit $\tau \to \infty$ and $|\nu| \gg 1$, where the polarization interaction becomes negligible, we obtain from equations (3.4) and (3.5) the limiting behavior of $\tilde{J}$:

$$\tilde{J}(\nu < 0) \to \left(1 - \frac{\nu}{\tau}\right) , \quad (4.17)$$

$$\tilde{J}(\nu > 0) \to \exp(-\nu/\tau) . \quad (4.18)$$

If we write

$$\langle Z\rangle \to \psi\tau \quad (4.19)$$

then ψ is the solution to the transcendental equation obtained by Spitzer (1941):

$$1 - \psi = \mu^{1/2}(m_p/m_e)^{1/2}e^{\psi} . \quad (4.20)$$

For a plasma with $\mu = 1$ (e.g., an electron-proton plasma with $s_e = 1$) one has $\psi = -2.504$, while $\psi = -3.799$ for a "heavy-ion" plasma with $\mu = 25$.

The dispersion σ_Z of the Gaussian is easily shown to be

$$\sigma_Z \to \left(\frac{1-\psi}{2-\psi}\right)^{1/2} \tau^{1/2} = \left[\frac{(1-\psi)}{(2-\psi)(-\psi)}\right]^{1/2} \langle -Z\rangle^{1/2} . \quad (4.21)$$

c) *Charge Distribution Functions*

Grain charge distribution functions have been computed numerically for the case of a plasma with $\mu = 1$, as well as the case of a "heavy-ion" plasma with $\mu = 25$. In Figures 5–10 we show results for $\tau = 0.1$, 0.3, 1, 3, 10, and 10^2. At low temperatures $\tau \lesssim 0.2$, the charge distribution is strongly concentrated in the -1 and 0 states, as expected from equations (4.9)–(4.14). At high temperatures $\tau \gtrsim 10$, the charge distribution begins to approximate the Gaussian distribution (4.15).

V. DISCUSSION

a) *Grain Size Distribution*

Below we will consider various phenomena which depend on the size distribution of the grains. Although the appropriate integrations over the size distribution are readily performed for any particular distribution of interest, it will be useful to adopt a particular distribution for purposes of illustration. Here we review briefly the available evidence pertaining to the size distribution of interstellar dust.

A graphite-silicate grain mixture with the MRN power law size distribution (Mathis, Rumpl, and Nordsieck 1977)

$$\frac{dn_{gr}}{da} = n_H A a^{-3.5} , \quad a_{min} < a < a_{max} , \quad (5.1)$$

with $a_{max} \approx 0.25$ μm, $a_{min} \lesssim 100$ Å, and $A = 1.5 \times 10^{-25}$ cm$^{2.5}$ has been found to be consistent with the "average" extinction law determined for diffuse interstellar clouds, as well as observations of interstellar polarization (Mathis, Rumpl, and Nordsieck 1977; Mathis 1979; Mathis and Wallenhorst 1981; Draine and Lee 1984; Mathis 1986). Unfortunately, existing

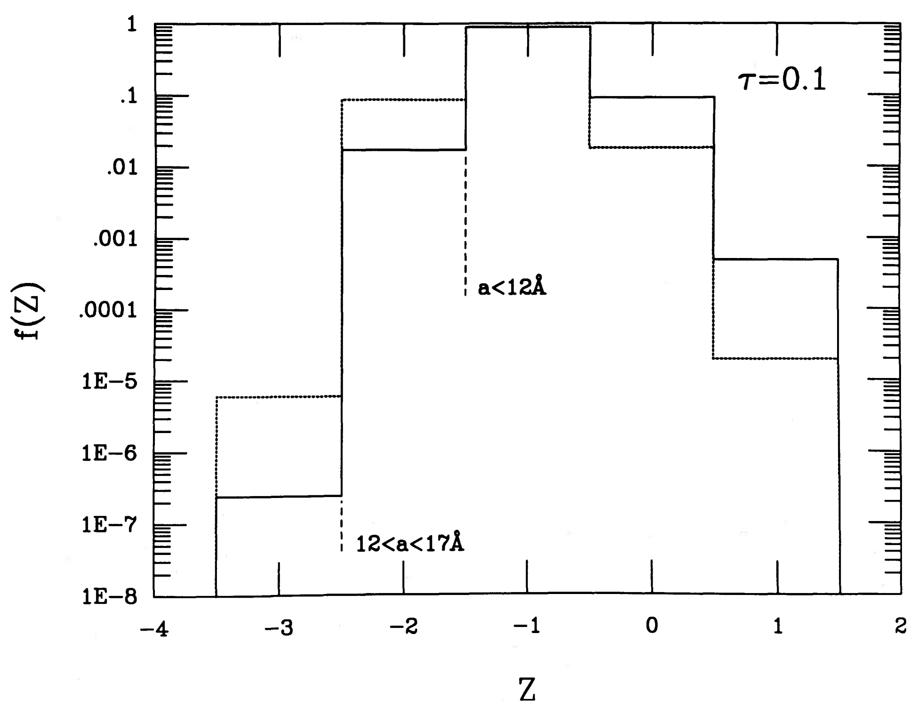

FIG. 5.—The charge distribution function $f(Z)$ for a grain in a plasma. Results are shown for $\mu = 1$ (*solid histogram*) and $\mu = 25$ (*dotted histogram*), where μ is the "effective atomic weight" of the ions, defined by eq. (4.8b). Results shown here are for "reduced temperature" $\tau = 0.1$, i.e., $aT = 1.67$ μm K, where a is the grain radius and T is the kinetic temperature of the plasma. For very small grains, the distribution function must be truncated, as indicated: e.g., an $a < 12$ Å grain with a charge $Z = -2$ will spontaneously emit an electron.

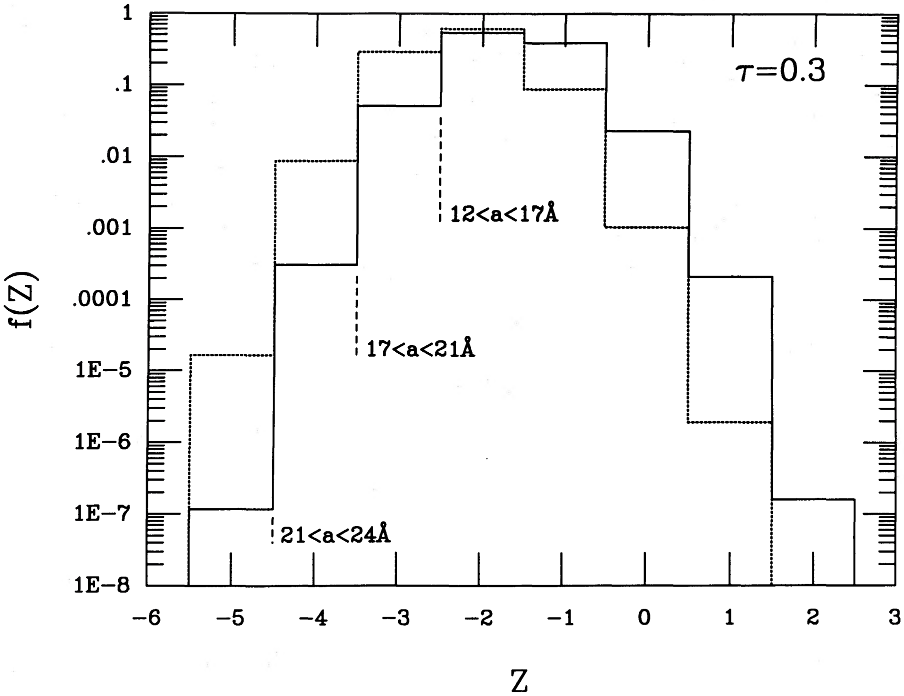

FIG. 6.—Same as Fig. 5, but for $\tau = 0.3$ (i.e., $aT = 5.01$ μm K). As in Fig. 5, results are shown for $\mu = 1$ (*solid histogram*) and $\mu = 25$ (*dotted histogram*).

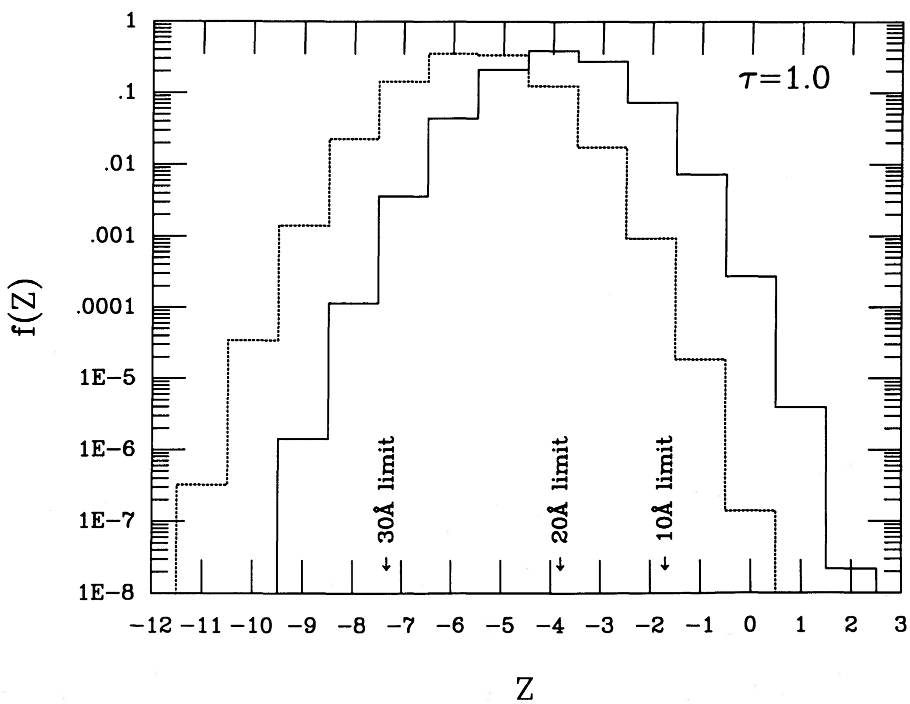

FIG. 7.—Same as Fig. 5, but for $\tau = 1$ (i.e., $aT = 16.7$ μm K). Results are shown for $\mu = 1$ (*solid histogram*) and $\mu = 25$ (*dotted histogram*). The limit (4.1) on Z is indicated for $a = 10$, 20, and 30 Å grains.

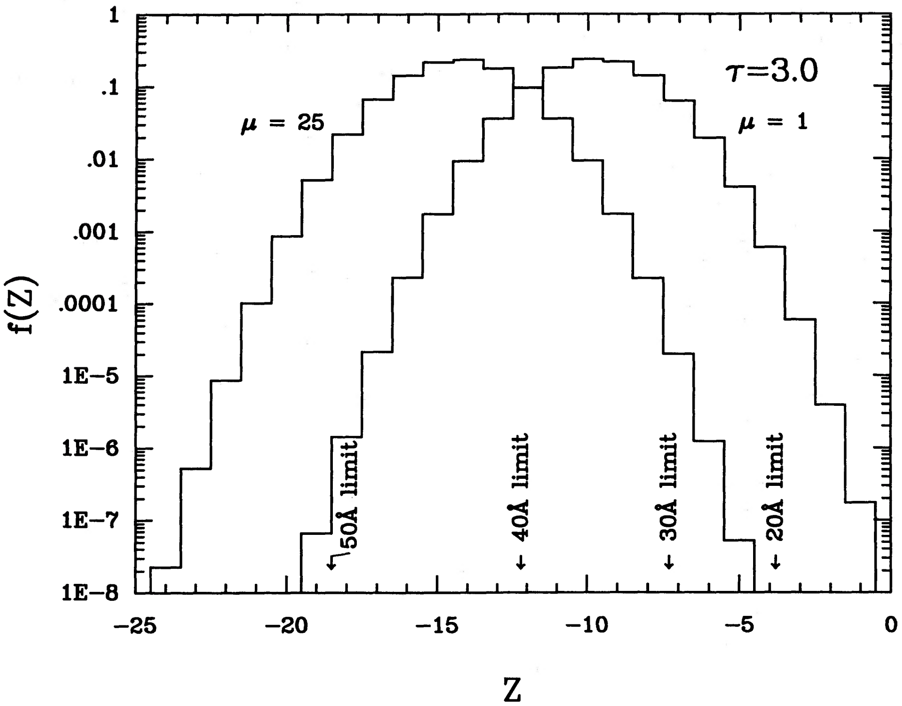

FIG. 8.—Same as Fig. 5, but for $\tau = 3$ (i.e., $aT = 50.1\ \mu$m K)

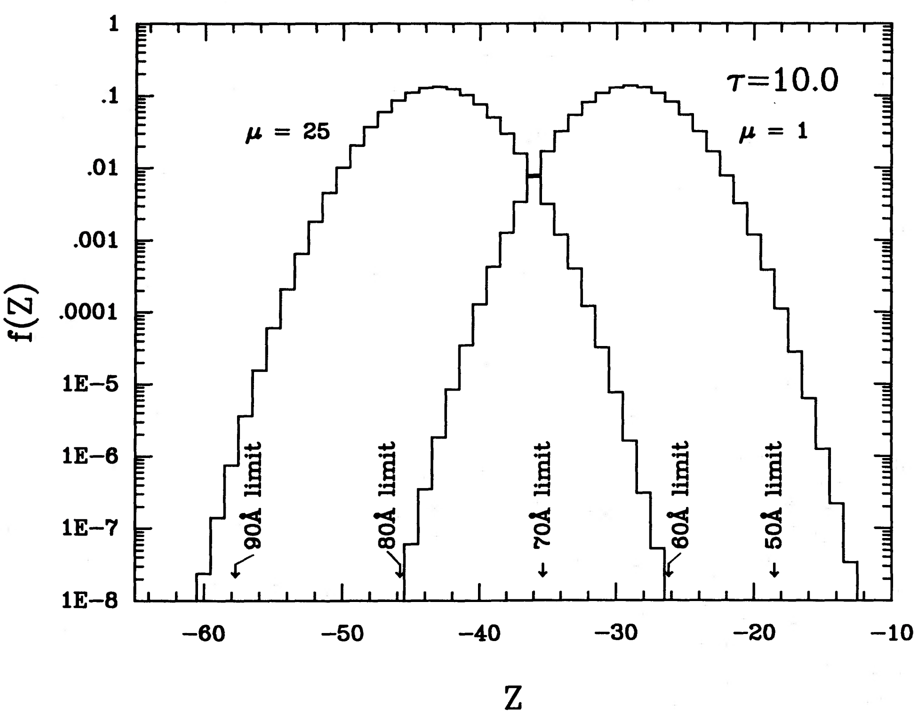

FIG. 9.—Same as Fig. 5, but for $\tau = 10$ (i.e., $aT = 167.\ \mu$m K)

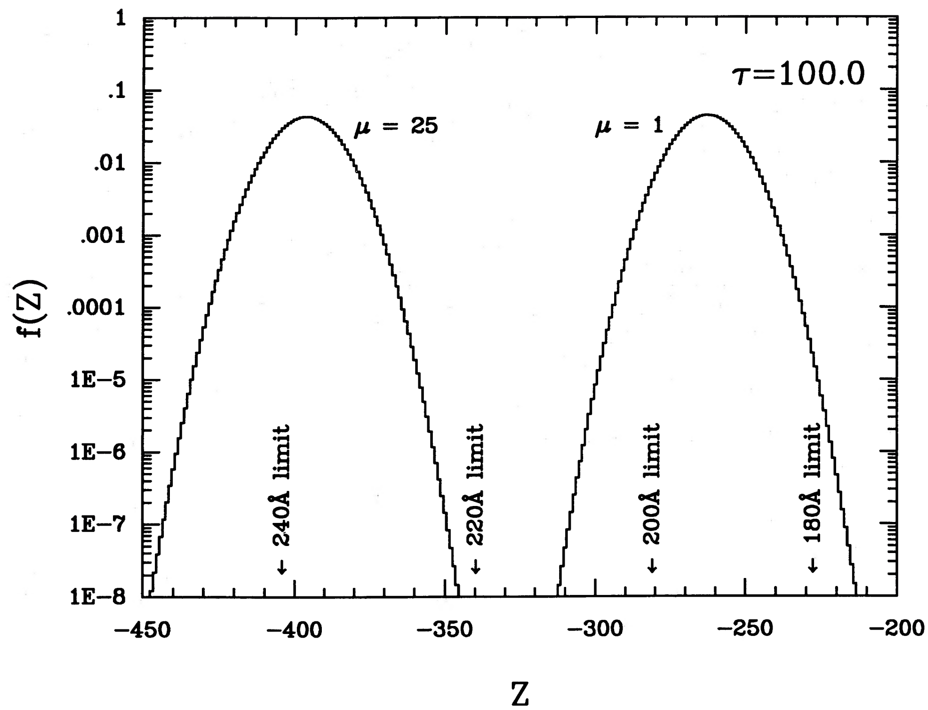

FIG. 10.—Same as Fig. 5, but for $\tau = 10^2$ (i.e., $aT = 1670\ \mu$m K)

extinction observations ($\lambda > 912$ Å) do not strongly constrain the value of the lower cutoff $a_{\rm min}$ for this distribution.

The strongest evidence regarding abundances of $a \lesssim 100$ Å particles originates from (1) observations of the unidentified infrared ("UIR") emission bands at $\lambda = 3.28$, 3.4, 6.2, 7.7, 8.6, and 11.3 μm from various planetary nebulae, reflection nebulae, and H II regions (see the reviews by Allamandola 1984 and Willner 1984), (2) observations of 1.25–4.8 μm continuum emission from reflection nebulae (Sellgren, Werner, and Dinerstein 1983), and (3) *IRAS* observations of diffuse clouds, initially at 60 and 100 μm (Low *et al.* 1984) and subsequently at 12 and 25 μm (Boulanger, Baud, and van Albada 1985; Weiland *et al.* 1986), revealing considerably more emission than originally expected at 60, 25, and 12 μm. Sellgren (1984) suggested that the near-infrared emission from reflection nebulae was simply thermal emission from very small grains undergoing temperature fluctuations, and Leger and Puget (1984) showed that thermal fluctuations in very small grains (=molecules) with the structure of polycyclic aromatic hydrocarbons ("PAHs") could explain the UIR features. Puget, Leger, and Boulanger (1985) and Draine and Anderson (1985) considered the continuum infrared emission from small grains. Draine and Anderson (1985) showed that the temperature fluctuations in small particles could produce the excess 60 μm emission observed by *IRAS*, and predicted that *IRAS* should detect 12 μm and 25 μm emission from diffuse clouds.

In Table 2 we show the predicted emission for grains with the MRN size distribution extended down to $a_{\rm min} = 3$ Å. This size distribution, with $a_{\rm max} = 0.25\ \mu$m, has 3% of the grain mass contributed by particles with $3 < a < 10$ Å (grains containing between 11 and 420 atoms if $\rho/m = 10^{23}$ cm^{-3}). Also shown in Table 2 are the *IRAS* observations of Boulanger, Baud, and van Albada (1985) and Weiland *et al.* (1986). We see that the observed 60 and 100 μm fluxes are in very good agreement with the model calculations, whereas the observed emission at 12 and 25 μm is even stronger than predicted for this "extended" MRN model. This strongly suggests that the smallest ($3 \lesssim a \lesssim 10$ Å) grains are even more abundant than the extended MRN distribution would imply. This same conclusion is reached from modelling of the UIR features as emission from PAHs: Leger and Puget (1984) estimated that PAHs had to contain 1.5%–6% of the cosmic carbon abundance.

We will therefore adopt the "extended" MRN size distribution (with $a_{\rm min} = 3$ Å) for purposes of illustration below, recognizing that interstellar diffuse clouds are likely to have even greater abundances of very small grains. Unfortunately, at the present time we have little knowledge of the abundances of small grains in dark clouds.

As noted above, estimates of the numbers of very small grains are based on theoretical modeling of temperature excursions following photon absorptions, phenomena which depend mainly on the number of atoms in the grain, and therefore constrain the grain *mass* distribution. Our assumption of spherical grains therefore *minimizes* the grain surface area and will tend to *underestimate* the rates for collisional processes.

b) *Average Grain Charge*

The charge on an individual dust grain fluctuates, with a time-averaged value

$$\langle Z \rangle = \sum_{-\infty}^{\infty} Z f(Z) . \tag{5.2}$$

At low temperatures, we may use equations (4.12)–(4.14) to obtain an analytic estimate for $\langle Z \rangle$, valid for $\tau \lesssim 0.2$ (where $\tau \equiv akT/e^2$):

$$\langle Z \rangle \approx \frac{-1}{1 + (\tau_0/\tau)^{1/2}} . \tag{5.3}$$

This may be combined with the high-temperature result (4.19)

TABLE 2

COMPARISON OF EXTENDED MRN MODEL WITH *IRAS* OBSERVATIONS

MODEL/OBSERVATION	$[\nu I_\nu]_\lambda/[\nu I_\nu]_{100\,\mu m}$ 12 μm	25 μm	60 μm	$I_\nu(100\ \mu m)/N_H$ (10^{-20} MJy sr^{-1} H^{-1})
MRN model, $\chi = 1$[a]	0.04	0.06	0.29	0.87
Cloud A[b]	...	...	0.50	1.64
Cloud B[b]	...	...	0.31	0.86
Cloud C[b]	...	...	0.26	0.33
Cloud D[b]	...	...	0.34	0.98
BBvA cirrus[c]	0.25 ± 0.06	0.15 ± 0.03	0.32 ± 0.04	1.1 ± 0.1
Cloud 16[d]	$0.24^{+0.25}_{-0.13}$	0.09 ± 0.03	0.28 ± 0.06	$1.2^{+1.2}_{-0.6}$[e]
Cloud 20[d]	0.41 ± 0.15	0.15 ± 0.06	0.29 ± 0.10	0.54 ± 0.31[e]

[a] Graphite-silicate mixture with MRN size distribution extended down to $a_{min} = 3$ Å, heated by average starlight (Draine and Anderson 1985).

[b] Low *et al.* 1984.

[c] Boulanger, Baud, and van Albada 1985.

[d] Weiland *et al.* 1986.

[e] Assuming $N_H = 1.87 \times 10^{21} A_V$ cm^{-2}.

to give the general approximation

$$\langle Z \rangle \approx \frac{-1}{1 + (\tau_0/\tau)^{1/2}} + \psi\tau\ . \tag{5.4}$$

In Figure 11 we plot our numerical results for $\langle Z \rangle$, together with the approximate formula (5.3), for both a proton-electron plasma and a heavy-ion plasma. The approximation (5.3) is seen to compare well with the exact numerical solutions.

In cold clouds with very low fractional ionizations, charged dust grains may carry an appreciable fraction of the free charge. At the low temperatures of interest, charged dust grains contribute a charge density

$$n_I - n_e \approx \int_{a_{min}}^{a_{max}} da\, \frac{dn_{gr}}{da} \left[\frac{1}{1 + (a_0/a)^{1/2}} - \frac{\psi a k T}{e^2}\right] \tag{5.5}$$

where

$$a_0 \equiv \frac{e^2\tau_0}{kT} = 0.463\ \text{Å} \left(\frac{20\ \text{K}}{T}\right)\left(\frac{25}{\mu}\right). \tag{5.6}$$

Note that a_0 is normally smaller than the smallest grains of interest (in cold regions where $T \lesssim 40$ K, we expect the ionization to be primarily due to heavy ions with $\mu \gtrsim 5$).

If we adopt the extended MRN size distribution (5.1), with $a_{min} \ll a_{max}$, the result may be accurately approximated by

$$\frac{n_I - n_e}{n_H} \approx \frac{2A}{5} \frac{a_{min}^{-2.5}}{1 + (4/5)(a_0/a_{min})^{1/2}} - \frac{2A\psi kT}{3e^2} a_{min}^{-1.5} \tag{5.7}$$

$$\approx 3.8 \times 10^{-7}\left(\frac{a_{min}}{3\ \text{Å}}\right)^{-2.5} + 6.9 \times 10^{-10}\left(\frac{-\psi}{3}\right)\left(\frac{T}{20\ \text{K}}\right)\left(\frac{a_{min}}{3\ \text{Å}}\right)^{-1.5}. \tag{5.8}$$

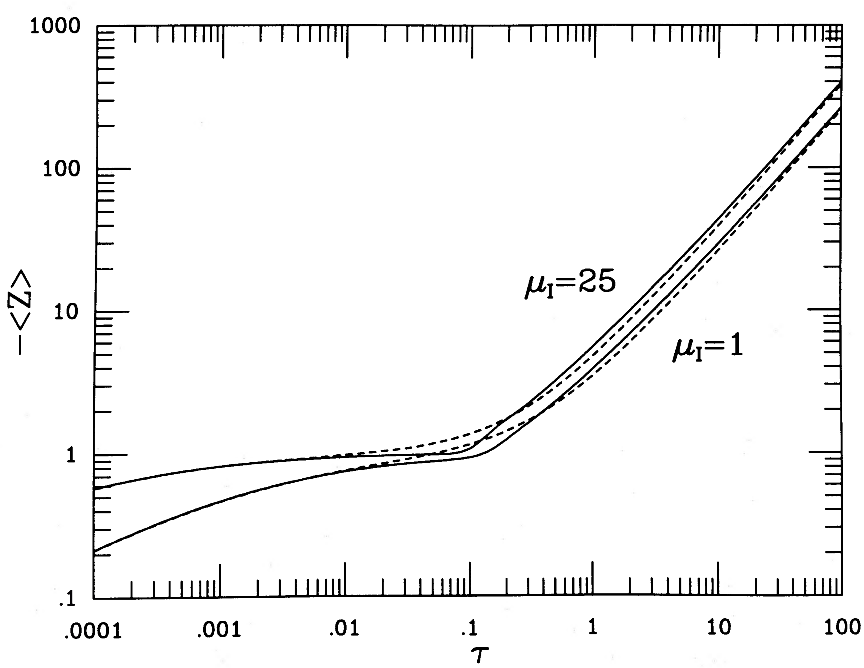

FIG. 11.—The mean charge $\langle Z \rangle$ on a grain, as a function of the reduced temperature $\tau = akT/e^2$. Results are shown for both $\mu = 1$ and $\mu = 25$, where μ is the "effective atomic weight" of the ions, defined by eq. (4.8b). Also plotted (*broken lines*) is the approximation (5.4).

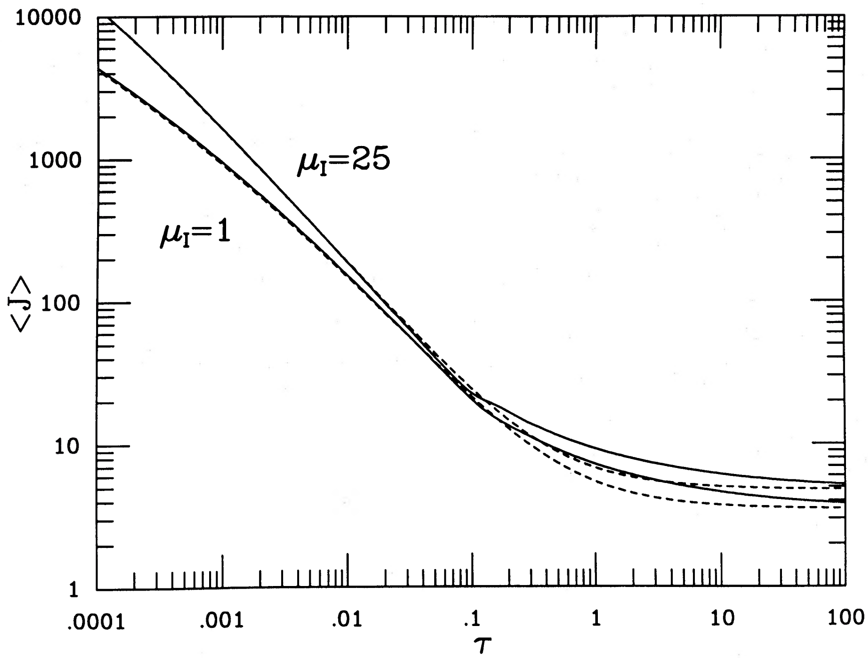

FIG. 12.—The mean reduced collision rate $\langle \tilde{J} \rangle$, as a function of the reduced temperature $\tau = akT/e^2$, for $\mu = 1$ and $\mu = 25$. Also plotted (*broken lines*) is the approximation (5.12).

We see that grains may carry a significant fraction of the grain charge in cold clouds of fractional ionization $n_e/n_H \lesssim 10^{-6}$ if ultrasmall grains are as abundant as they appear to be in the diffuse interstellar medium. If the smallest grains are appreciably nonspherical, then the trapped charge on the grains will be even greater than given by equation (5.8). Note that the results are nearly independent of μ, the "effective" atomic weight of the ions: the leading term in equation (5.8) has no dependence on μ, while the remaining term depends only weakly on μ, since $2.5 < -\psi < 3.8$ for $1 < \mu < 25$.

c) *Electron-Ion Recombination on Grains*

In dense molecular clouds of low fractional ionization, collisions of electrons and ions with grains becomes an important recombination process. Since the number density of dust grains n_{gr} is proportional to n_H, we may write the rate of recombination of ions by this process as $dn_i/dt = -\alpha_{gr} n_H n_i$, where n_H is the number density of H nuclei. Let m_i be the mass of a particular ion species of interest, assumed to have charge $+1$. The effective recombination rate coefficient α_{gr} is then

$$\alpha_{gr} = \int_{a_{min}}^{a_{max}} da\, a^2 \frac{1}{n_H}\frac{dn_{gr}}{da}\left(\frac{8\pi kT}{m_i}\right)^{1/2}\left\langle \tilde{J}\left(\tau = \frac{akT}{e^2}\right)\right\rangle \quad (5.9)$$

where

$$\langle \tilde{J}(\tau) \rangle \equiv \sum_{Z=-\infty}^{\infty} \tilde{J}(\tau, Z) f(Z)\,. \quad (5.10)$$

In Figure 12 we plot numerically-computed values of $\langle \tilde{J} \rangle$ as a function of τ. For $\tau \lesssim 0.2$, when most of the grains have charges $Z = -1$ or 0, equations (4.10)–(4.11) may be used to obtain the analytic result

$$\langle \tilde{J} \rangle \approx \frac{2/\tau}{1 + (\tau_0/\tau)^{1/2}}\,. \quad (5.11)$$

For $\tau \to \infty$ we have $\tilde{J} \to (1 - \psi)$, so a satisfactory general approximation is provided by

$$\langle \tilde{J} \rangle \approx \frac{2/\tau}{1 + (\tau_0/\tau)^{1/2}} + (1 - \psi)\,. \quad (5.12)$$

The approximation (5.12) is plotted in Figure 12 and is seen to provide a satisfactory approximation for all τ.

The low-temperature grain recombination rate coefficient may thus be estimated from equation (5.12) to be

$$\alpha_{gr} \approx \left(\frac{32\pi}{m_i kT}\right)^{1/2} e^2 \int_{a_{min}}^{a_{max}} da\, a \frac{1}{n_H}\frac{dn_{gr}}{da}\frac{1}{1 + (a_0/a)^{1/2}} + \left(\frac{8\pi kT}{m_i}\right)^{1/2}(1 - \psi)\int_{a_{min}}^{a_{max}} da\, a^2 \frac{dn_{gr}}{da}\,, \quad (5.13)$$

where a_0 is defined by equation (5.6). For the MRN power-law size distribution (5.1) with $a_{min} \ll a_{max}$ one obtains

$$\alpha_{gr} \approx \frac{8}{3} Ae^2 a_{min}^{-1.5}\left(\frac{2\pi}{m_i kT}\right)^{1/2}\left[1 + \frac{2}{3}\left(\frac{a_0}{a_{min}}\right)^{1/2}\right]^{-1} + \left(\frac{32\pi kT}{m_i}\right)^{1/2}(1 - \psi)Aa_{min}^{-0.5} \quad (5.14)$$

$$= 1.3 \times 10^{-13}\ \mathrm{cm^3\ s^{-1}}\left(\frac{a_{min}}{3\ \text{Å}}\right)^{-3/2}\left(\frac{20}{T}\right)^{1/2}\left(\frac{25 m_H}{m_i}\right)^{1/2} \times \left[1 + 2.2 \times 10^{-3}\left(\frac{a_{min}}{3\ \text{Å}}\right)\left(\frac{T}{20}\right)\left(\frac{1 - \psi}{4}\right)\right], \quad (5.15)$$

where we have assumed $a_0 \ll a_{min}$. The effective recombination coefficient will be even greater if the smallest grains are appreciably nonspherical (cf. § Va). Once again the results are very weakly dependent on the "effective" atomic weight μ of the ions, since this enters only through the dependence on ψ, and $2.5 < -\psi < 3.8$ for $1 < \mu < 25$.

This result (5.15) for α_{gr} is approximately three orders of magnitude greater than the estimates of Umebayashi and Nakano (1980). In part this is due to differences in the assumed grain size distribution (we have assumed greater numbers of very small grains), but most of the difference can be attributed to the effect of the polarization interaction.

Since the rate coefficient for radiative recombination of metal ions at temperatures $T \approx 20$ K is typically $\alpha_{rr} \approx 1.6 \times 10^{-11}(T/20)^{-1/2}$ cm^3 s^{-1} (Gould 1978), our result (5.14) implies that recombination on grains having the MRN distribution would dominate radiative recombination when $n_e/n_H \lesssim 10^{-2}(a_{min}/3\ \text{Å})^{-3/2}$. In fact, even species subject to fast dissociative recombination (e.g., HCO^+, with a rate coefficient $\alpha_{dr} \approx 1.5 \times 10^{-6}(T/20)^{-0.75}$ cm^3 s^{-1} [Mitchell and McGowan 1983]) may recombine more rapidly with grains when $n_e/n_H \lesssim 10^{-7}(a_{min}/3\ \text{Å})^{-3/2}$ (recall also that the grains may deplete the number of free electrons at these levels of fractional ionization). Evidently recombination on grains may be *extremely* important in dark clouds, at least until the numbers of small grains are suppressed (by many orders of magnitude) below their abundances in diffuse clouds. Omont (1986) has reached a similar conclusion for PAHs, for which (assuming 1.5% of the cosmic carbon abundance to be in PAHs) he estimates an effective recombination rate coefficient $\alpha_{PAH} \approx 2 \times 10^{-14}$ cm^3 s^{-1} $(20/T)^{1/2}(25m_H/m_i)^{1/2}$.

The important ion $H_3{}^+$ is now thought not to be subject to dissociative recombination when in its ground vibrational state: Adams and Smith (1986) have measured an upper limit $\alpha < 10^{-11}$ cm^3 s^{-1} for the recombination rate coefficient for $H_3{}^+$ at $T = 80$ K. This reduction in the recombination rate for $H_3{}^+$ has been taken to imply a significant increase in the abundance of $H_3{}^+$ in dark clouds, relative to the abundance which had been estimated assuming dissociative recombination to be rapid. Such an enhanced abundance of $H_3{}^+$ would have a number of important chemical consequences, including, for example, an increased rate of formation of HCO^+ by the reaction $CO + H_3{}^+ \rightarrow HCO^+ + H_2$. While our ignorance of the grain size distribution in dark clouds precludes an accurate estimate, we note that *if* the MRN size distribution applies, then recombination on small grains may provide an important destruction channel for $H_3{}^+$, with a rate coefficient $\alpha_{gr} \approx 3.8 \times 10^{-13}$ cm^3 s^{-1} $(a_{min}/3\ \text{Å})^{-3/2}$ at $T = 20$ K; this rate coefficient leads to $H_3{}^+$ recombination at a rate comparable to charge transfer to or reaction with "metal" atoms such as atomic oxygen (taking the "metal" atom abundance to be 2×10^{-4} and the rate coefficient to be $\sim 2 \times 10^{-9}$ cm^3 s^{-1}).

VI. SUMMARY

1. We have computed the energy-dependent cross section for a charged particle to collide with a charged, conducting sphere. This cross section is a good approximation to the cross section for charged dielectric spheres with $\epsilon \gtrsim 5$.

2. We have obtained thermal rate coefficients for collisions of charged particles with charged, conducting spheres. These rate coefficients depend upon two dimensionless parameters: the ratio ν of the grain charge Ze to the charge q on the incident particles, and the "reduced temperature" $\tau \equiv akT/q^2$. In addition to numerical results, we provide simple analytic approximations [eq. (3.4) and (3.5)] for these rate coefficients.

3. Charge distribution functions $f(Z)$, giving the fraction of grains in different charge states Z, have been computed for various values of τ, in the limit of pure collisional charging (photoelectric emission is neglected). The charge distribution functions depend on only two dimensionless parameters: the "reduced temperature" τ, and the "effective atomic weight" μ of the ions, defined by eq. (4.8b); μ depends not only on the actual masses of the ions, but also on the electron sticking coefficient s_e and the ratio n_e/n_I of the electron and ion number densities. For $\tau < \tau_0$, the grains are mostly neutral, where τ_0 is given by equation (4.14). The polarization interaction with free electrons causes the grains to be primarily in charge state $Z = -1$ for $\tau_0 < \tau \lesssim 0.2$. For $\tau \gtrsim 1$, the mean grain charge is approximated by $\langle Z \rangle = \psi\tau$, where $\psi = -2.504$ for $\mu = 1$ and $\psi = -3.799$ for a "heavy-ion" plasma with $\mu = 25$.

4. If the MRN power law, extended down to $a_{min} \approx 3$ Å, is adopted for the grain size distribution, then it is found that grains in cold clouds may trap an appreciable fraction of the free electrons when $n_e/n_H \lesssim 4 \times 10^{-7}$.

5. For the extended MRN size distribution, ion recombination on grains is faster than radiative recombination for $n_e/n_H \lesssim 10^{-2}$, and faster than even dissociative recombination for $n_e/n_H \lesssim 10^{-7}$. At low temperatures ($T \lesssim 40$ K) species such as $H_3{}^+$ may be destroyed more rapidly by collisions with small grains than by reaction with metal atoms or molecules. This may have significant consequences for the ionization balance and chemistry within dense dark clouds.

This research was supported in part by grant AST 83-41412 from the National Science Foundation. It is a pleasure to thank L. Spitzer, Jr., and E. van Dishoeck for helpful discussions.

APPENDIX A

IMAGE POTENTIAL FOR DIELECTRIC SPHERES

The force acting on a charge q located a distance r from the center of a homogeneous sphere of dielectric constant ϵ may be derived from the interaction potential

$$\Phi(r) = \frac{qQ}{r} + \Phi_{im}(r)\,, \tag{A1}$$

where Φ_{im}, the "image potential" contribution arising from polarization of the dielectric sphere, is given by (Batygin and Toptygin 1978)

$$\Phi_{im}(r) = -\frac{(\epsilon - 1)}{2}\frac{q^2}{a}\sum_{l=1}^{\infty}\frac{l}{l\epsilon + l + 1}\left(\frac{a}{r}\right)^{2l+2}\,. \tag{A2}$$

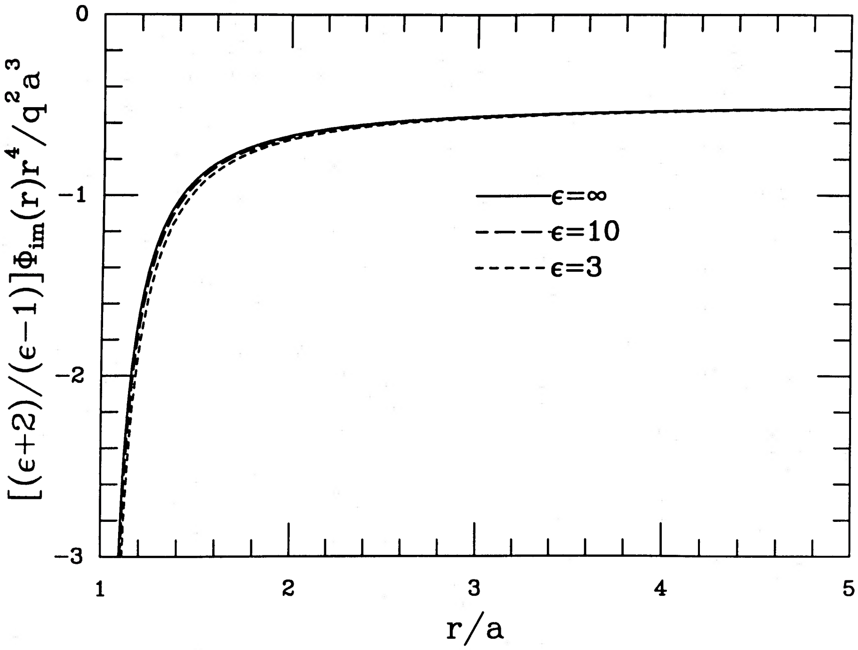

FIG. 13.—The scaled interaction potential for a point charge a distance r from a neutral homogeneous sphere of radius a (see Appendix A). Results are shown for dielectric spheres with $\epsilon = 3$ and 10, and for a conducting sphere ($\epsilon = \infty$). It is seen that the different values of ϵ have nearly the same functional form, except for a multiplicative factor $[(\epsilon - 1)/(\epsilon + 2)]$.

A surprisingly good approximation to $\Phi_{im}(r)$ is provided by

$$\Phi_{im}(r) \approx -\left(\frac{\epsilon - 1}{\epsilon + 2}\right) \frac{q^2 a^3}{2r^2(r^2 - a^2)} ; \tag{A3}$$

this approximation is asymptotically exact for $r \to \infty$, reduces to the exact solution for the conducting sphere as $\epsilon \to \infty$, and provides a very good approximation for general ϵ and r. The accuracy of this approximation may be seen in Figure 13, where we plot the rescaled potential $[(\epsilon + 2)/(\epsilon + 1)]\Phi_{im}(r)r^4/q^2a^3$ for $\epsilon = 3$, 10, and ∞. It is seen that these curves differ only slightly from one another, thus confirming that the polarization interaction for a dielectric sphere is essentially proportional to that for a conducting sphere, with the proportionality factor $[(\epsilon - 1)/(\epsilon + 2)]$. This proportionality factor exceeds 0.57 for $\epsilon > 5$. It is straightforward to show that at low temperatures ($\tau \equiv akT/e^2 \ll 1$) the rate coefficient for charged particle collisions with a neutral grain is reduced below the result for a neutral conducting sphere by the factor $[(\epsilon - 1)/(\epsilon + 2)]^{1/2}$, which exceeds 0.75 for $\epsilon > 5$. Thus the collisional charging of dielectric spheres with $\epsilon > 5$ will differ only in numerical detail from the results for a conducting sphere of the same radius.

APPENDIX B

COLLISION CROSS SECTION

Consider a particle with charge q and energy E_0, approaching a conducting sphere with charge Q and radius a. The interaction potential is (see eq. [2.1])

$$\Phi(r) = \frac{qQ}{r} - \frac{q^2 a^3}{2r^2(r^2 - a^2)} . \tag{B1}$$

Let b be the impact parameter. If the particle does not collide with the sphere, then there is a distance of closest approach r_{min}; conservation of energy and angular momentum gives the condition

$$E_0 = E_0\left(\frac{b}{r_{min}}\right)^2 + \Phi(r_{min}) . \tag{B2}$$

Define $x \equiv r_{min}/a$, $\beta \equiv b/a$, $\epsilon \equiv E_0 a/q^2$, $\nu \equiv Q/q$, and substitute equation (B1) into equation (B2) to obtain the condition on x for given β:

$$f(x, \beta) = g(x) , \tag{B3}$$

where

$$f(x, \beta) \equiv \nu x - \epsilon x^2 + \beta^2 \epsilon \tag{B4}$$

$$g(x) \equiv \frac{1}{2(x^2 - 1)} . \tag{B5}$$

It is easily seen graphically that the smallest value of β for which equation (B3) has a solution occurs for β such that f and g are tangent: $df/dx = dg/dx$, providing the additional equation

$$(2\epsilon x - \nu)(x^2 - 1)^2 + x = 0 . \tag{B6}$$

The root $x(\epsilon, \nu)$ of this equation determines the minimum value of $r_{\rm min}$; one can determine the corresponding impact parameter $b_{\rm crit} = \beta_{\rm crit}\, a$ by solving equation (B3) for β^2:

$$\beta^2 = x^2 + \frac{1}{\epsilon}\left[\frac{1}{2(x^2 - 1)} - \nu x\right] ; \tag{B7}$$

substituting $x(\epsilon, \nu)$ into equation (B7) gives $\beta_{\rm crit}$. The collision cross section is just $\pi b_{\rm crit}{}^2 = \pi a^2 \beta^2$.

REFERENCES

Adams, N. G., and Smith, D. 1986, in *IAU Symposium 120, Astrochemistry*, ed. M. S. Vardya and S. P. Tarafdar (Dordrecht: Reidel), p. 1.
Allamandola, L. J. 1984, in *Galactic and Extragalactic Infrared Spectroscopy*, ed. M. F. Kessler and J. P. Phillips (Dordrecht: Reidel), p. 5.
Batygin, V. V., and Toptygin, I. N. 1978, *Problems in Electrodynamics* (2d ed.; New York: Academic), p. 248.
Boulanger, F., Baud, B., and van Albada, G. D. 1985, *Astr. Ap.*, **144**, L9.
Draine, B. T., and Anderson, N. 1985, *Ap. J.*, **292**, 494.
Draine, B. T., and Lee, H. M. 1984, *Ap. J.*, **285**, 89.
Draine, B. T., and Sutin, B. 1987, in preparation.
Elmegreen, B. 1979, *Ap. J.*, **232**, 729.
Fredericks, W. J., and Cook, C. J. 1961, *Phys. Rev.*, **121**, 1693.
———. 1963, *J. Phys. Soc. Japan*, Vol. **18**, Suppl. 2, p. 281.
Gomer, R. 1961, *Field Emission and Field Ionization* (Cambridge: Harvard University Press).
Gould, R. J. 1978, *Ap. J.*, **219**, 250.
Havnes, O. 1984, *Adv. Space Res.*, Vol. **4**, No. 9, p. 75.
Hollenbach, D., and Salpeter, E. E. 1970, *J. Chem. Phys.*, **53**, 79.
Jackson, J. D. 1962, *Classical Electrodynamics* (New York: Wiley).
Lander, J. J., and Morrison, J. 1964, *J. Appl. Phys.*, **35**, 3593.
Leger, A., and Puget, J. L. 1984, *Astr. Ap.*, **137**, L5.
Low, F. J., *et al.* 1984, *Ap. J.* (*Letters*), **278**, L19.
Mathis, J. S. 1979, *Ap. J.*, **232**, 747.
———. 1986, *Ap. J.*, **308**, 281.
Mathis, J. S., Rumpl, W., and Nordsieck, K. H. 1977, *Ap. J.*, **217**, 425.
Mathis, J. S., and Wallenhorst, S. G. 1981, *Ap. J.*, **244**, 483.
Mestel, L., and Spitzer, L., Jr. 1956, *M.N.R.A.S.*, **116**, 503.
Mitchell, J. B. A., and McGowan, J. W. 1983, in *The Physics of Ion-Ion and Electron-Ion Collisions*, ed. F. Brouillard and J. W. McGowan (New York: Plenum), p. 279.
Muller, E. W., and Tsong, T. T. 1969, *Field Ion Microscopy* (New York: American Elsevier).
Nakano, T. 1976, *Pub. Astr. Soc. Japan*, **28**, 355.
Nakano, T., and Tademaru, E. 1972, *Ap. J.*, **173**, 87.
Nakano, T., and Umebayashi, T. 1980, *Pub. Astr. Soc. Japan*, **32**, 613.
Omont, A. 1986, *Astr. Ap.*, **164**, 159.
Puget, J. L., Leger, A., and Boulanger, F. 1985, *Astr. Ap.*, **142**, L19.
Sellgren, K. 1984, *Ap. J.*, **277**, 623.
Sellgren, K., Werner, M. W., and Dinerstein, H. L. 1983, *Ap. J.* (*Letters*), **271**, L13.
Spitzer, L. 1941, *Ap. J.*, **93**, 369.
Touloukian, Y. S., and Ho, C. Y. 1981, *Physical Properties of Rocks and Minerals*, Vol. **2** (New York: McGraw-Hill).
Umebayashi, T., and Nakano, T. 1980, *Pub. Astr. Soc. Japan*, **32**, 405.
Watson, W. D. 1974, *Ap. J.*, **188**, 35.
Weiland, J. L., Blitz, L., Dwek, E., Hauser, M. Magnani, L., and Rickard, L. J. 1986, *Ap. J.* (*Letters*), **306**, L101.
Willner, S. P. 1984, in *Galactic and Extragalactic Infrared Spectroscopy*, ed. M. F. Kessler and J. P. Phillips (Dordrecht: Reidel), p. 37.

B. T. DRAINE and BRIAN SUTIN: Princeton University Observatory, Peyton Hall, Princeton, NJ 08544